Wavespeed selection of travelling wave solutions of a two-component reaction-diffusion model of cell invasion

Yuhui Chen[*]   Michael C. Dallaston[*†]

November 20, 2024

Abstract

We consider a two-component reaction-diffusion system that has previously been developed to model invasion of cells into a resident cell population. This system is a generalisation of the well-studied Fisher–KPP reaction diffusion equation. By explicitly calculating families of travelling wave solutions to this problem, we observe that a general initial condition with either compact support, or sufficiently large exponential decay in the far field, tends to the travelling wave solution that has the largest possible decay at its front. Initial conditions with sufficiently slow exponential decay tend to those travelling wave solutions that have the same exponential decay as their initial conditions. We also show that in the limit that the (nondimensional) resident cell death rate is large, the system has similar asymptotic structure as the Fisher–KPP model with small cut-off factor, with the same universal (leading order) logarithmic dependence on the large parameter. The asymptotic analysis in this limit explains the formation of an interstitial gap (a region preceding the invasion front in which both cell populations are small), the width of which is also logarithmically large in the cell death rate.

1 Introduction

Systems of reaction-diffusion partial differential equations (PDEs) have been used to model the interaction of species in ecology, biology and chemistry since the pioneering

---

[*]School of Mathematical Sciences, Queensland University of Technology, Brisbane QLD 4000, Australia

[†]Corresponding author: `michael.dallaston@qut.edu.au`

work of Fisher [13] and Kolmogorov et al. [17]. The canonical example is the Fisher–KPP equation, which couples linear diffusion with logistic growth, and may be written (nondimensionally) as

$$\frac{\partial u}{\partial t} = \frac{\partial^2 u}{\partial x^2} + u(1 - u). \tag{1}$$

The most widely-studied property of the Fisher–KPP equation (1) is that a localised initial condition on an unbounded spatial domain will evolve to a travelling wave solution, by which the solution transitions from the unstable state $u = 0$ to the stable state $u = 1$. It is well known that, for an exponentially decaying initial condition $u \sim e^{-ax}$, $x \to \infty$, the travelling wave (with associated wave speed c) that is selected is the one that has the same exponential decay rate, if such a solution exists, or the one with maximum decay rate $a = 1$ otherwise [1, 2]. This selection implies that the wave speed is given by

$$c = \begin{cases} 2 & a \geq 1 \\ a + \dfrac{1}{a} & a < 1. \end{cases}$$

A compactly supported initial condition (which may be thought of as the limiting case $a \to \infty$) tends to the travelling wave with minimum speed $c = 2$. It was established in Bramson [4] that, for a compactly supported initial condition, the rate at which the travelling wave speed is approached is logarithmic; if $x_f(t)$ is the spatial location of a characteristic point on the wave (for example, the point at which $u = 1/2$), then

$$x_f = 2t - \frac{3}{2} \log t + O(1), \qquad t \to \infty. \tag{2}$$

(see also Hamel et al. [16], Nolen et al. [19]). As well as of inherit interest, this slow convergence is important to take into account when trying to estimate the long-time wave speed from numerical simulations.

Many extensions to the Fisher–KPP equation (1) have been considered, with particular focus on the resulting wave speed of travelling wave solutions. A modification of the reaction term in (1) to have a small 'cut-off' was considered in Brunet and Derrida [6]:

$$\frac{\partial u}{\partial t} = \frac{\partial^2 u}{\partial x^2} + u(1 - u)f(u; \epsilon), \qquad f(u; \epsilon) = \begin{cases} 1 & u > \epsilon \\ 0 & u \leq \epsilon \end{cases}, \tag{3}$$

where $\epsilon \ll 1$. The motivation behind this cut-off term comes from considering (1) as the continuous limit of a discrete process, where ϵ represents the discrete cell size. The matched asymptotic analysis in [6] established that the correction to the wave speed in the limit $\epsilon \to 0$ was logarithmic:

$$c \sim 2 - \frac{\pi^2}{(\log \epsilon)^2}, \qquad \epsilon \to 0, \tag{4}$$

2

and that this correction was universal for a more general class of cut-off functions. The matched asymptotic argument has more recently been made rigorous using geometric singular perturbation theory in Dumortier et al. [10].

To model more complex biological processes such as tumour growth, in which multiple cell or chemical species may be involved, systems of multiple reaction-diffusion models have been developed and analysed. Gatenby and Gawlinski [15] developed a three-species model of tumour growth under the acid-mediation hypothesis, in which an invading cell population increases the acidity of the environment (modelled by the production and diffusion of H^+ ions), which then negatively impacts the resident (non-diffusive) healthy cell population [21, 3]. In this model, the diffusivity of the invading cells is assumed to be a decreasing function of the resident cell population, such that when the healthy cell population is at capacity, the diffusivity vanishes. The decrease in resident cell population due to acidity is thus required to allow the tumour to grow.

In Gatenby and Gawlinski [15] it was numerically observed that solutions to their three-component model tend to travelling wave solutions as time increases. A particular point of interest was that when the death of resident cells due to acidity was large, there was a separation between the advancing front of invading cells and receding front of resident cells, in which both cell populations were small. This region is referred to as the hypocellular *interstitial gap*, and was observed in experimental observations. Gatenby and Gawlinski [15] estimated that the size of this region was logarithmically large in the dimensionless resident cell death rate. The asymptotic analysis of travelling wave solutions has also been carried out more recently in Fasano et al. [12], Davis et al. [8]; the interstitial gap is a feature of waves that have speed $O(1)$ in the limit that acid diffusivity is much larger than the cell diffusivity (referred to as 'slow' waves in Fasano et al. [12], Davis et al. [8], the 'fast' waves relating to the finite diffusivity of the acid species).

Simplified versions of the three-species model of Gatenby and Gawlinski [15] have been studied, by neglecting the acid species, and directly modelling the effect of resident cell population on the diffusivity of the invading species. Gallay and Mascia [14] show that travelling wave solutions exist for any wavespeed c, while Mascia et al. [18] describe numerical solution methods. The stability of travelling wave solutions was considered in Swartwood [22], who show that all travelling waves are stable, regardless of the speed c (this is similar to the Fisher–KPP equation (1), where the marginal stability threshold is considered as the relevant wavespeed selection mechanism [23, 24]). Colson et al. [7] consider the case where in addition, resident cell species do not recover, and may initially be at less than the carrying capacity. In that study, families of travelling wave solutions are constructed in phase space by a shooting algorithm. A minimum wave speed is identified as a function of the resident cell death rate, and the initial resident cell population.

Recently, Browning et al. [5] and El-Hachem et al. [11] consider another version of a

simplified model of tumour growth whereby the two cell species react directly. In this model, both the diffusion and the carrying capacity of the invading cells is inhibited by the healthy cell population, and resident cells v do not proliferate, but are only destroyed by the invading species:

$$\frac{\partial u}{\partial t} = \frac{\partial}{\partial x}\left[(1-v)\frac{\partial u}{\partial x}\right] + u(1-u-v), \tag{5a}$$

$$\frac{\partial v}{\partial t} = -\gamma u v, \tag{5b}$$

In this model, u is the invading species, and v is the resident species. This model may be seen as a version of the system studied in Colson et al. [7] with an additional effect of v on the carrying capacity of u. Nominally this model has a single parameter, the dimensionless resident cell death rate γ, but since in this model there is no proliferation of v, the initial condition of v plays an important role. The diffusivity of u vanishes at $v = 1$, but the diffusion will only be degenerate if the initial condition takes this value. Although travelling wave solutions of (5) were observed in PDE simulations in El-Hachem et al. [11] over a range of parameter values and initial conditions, and the boundary value problem for travelling wave solutions was posed, the explicit computation of travelling wave solutions was not performed, and the mechanism by which the wave speed is determined by the parameters was not established.

In this article we consider the model (5). We explicitly calculate travelling wave solutions via numerical continuation over a large range of parameter values (in particular the resident cell death rate γ), and compare with time-dependent numerical simulations. We are thus able to numerically observe that, although the details of the phase space are more complicated, the principle by which the wave speed is selected is the same as for the simpler Fisher–KPP system: that is, an initial condition with sufficiently small exponential decay rate will tend to the travelling wave solution with the same decay rate (if it exists), and that an initial condition with compact support (or sufficiently large exponential decay) will tend to the travelling wave solution that has maximum decay rate. This is similar to the observation made in Colson et al. [7] for their simpler system.

In addition, our method of calculating travelling wave solutions allows us to compute solutions in the asymptotic limit as the resident cell death rate γ becomes large. We show that the asymptotic structure in this limit is very similar to that for the Fisher–KPP system with cut off (3), in which γ^{-1} plays the role of the small parameter ϵ. The leading order correction to the velocity is the same as the universal correction (4). We also find the next term in the correction, although this requires the numerical calculation of prefactors in each of the leading order problems in the asymptotic analysis. By carrying out a matched asymptotic expansion in this limit, we observe that the wave speed converges logarithmically to the (nondimensional) Fisher–KPP wave speed of $c = 2$. This asymptotic solution also explains why the model exhibits an interstitial gap where both cell populations are small; the width of this zone is also logarithmically

dependent on the cell death parameter. We show that the predictions made by the asymptotic analysis agree with the numerically computed travelling wave solutions.

2   Model and numerical PDE simulations

We start by describing the method and results of numerical simulations of the system (5). El-Hachem et al. [11] report on a large number of numerical simulations of this system; our aim here is to reproduce their main observations in order to confirm the validity of the travelling wave solutions in the next section. The system (5) comprises a population density of invading cells $u(x, t)$ invading a stationary population of resident cells $v(x, t)$, where both the diffusion and carrying capacity of the invading cells is negatively affected by the resident population. The nondimensional parameter γ in (5) represents the rate of destruction of resident cells, compared to the proliferation time scale; Browning et al. [5] and El-Hachem et al. [11] contain further details of this model, including the nondimensionalisation.

Initially, the domain consists of a spatially localised invading cell population $u_0(x)$ in a uniform resident cell population v_0:

$$u(x, 0) = u_0(x), \qquad v(x, 0) = v_0. \tag{6}$$

Note that if $v_0 = 0$ identically, the system (5) reduces to the Fisher–KPP problem for u. In addition, the diffusivity vanishes when $v = 1$; in this paper, we will consider only $0 < v_0 < 1$, as our main focus is on the effects of v on the proliferation, rather than the effect of degenerate diffusion (see the discussion in Sect. 5).

To simulate (5) numerically, we discretise in space using a standard cell-centred finite volume method [20] with equally sized cells, and advance in time using the `ode15s` algorithm in MATLAB. To observe the formation of travelling wave behaviour, we consider a large spatial domain $x \in [0, L]$ with $L \gg 1$ approximating a semi-infinite domain, with zero flux conditions $(\partial_x u = 0)$ conditions imposed at the boundaries. A nonzero initial condition $u(x, 0)$ near $x = 0$ is then used to represent a localised initial condition. We generally choose $L \sim 150$–200 and $N \sim 10^4$ grid points, which is more than adequate for the numerical simulations to have converged.

We calculate the wave speed from PDE simulations by estimating the location of the travelling wave front $x_f(t)$ where $u(x_f(t), t) = 0.5$, interpolating the solution between neighbouring grid points if required. This calculation is sensitive in that sufficient time must have passed to minimise the effect of the initial condition, and the domain size L must be sufficiently large to minimise the effect of the right hand boundary. Rather than fit a simple linear function to x_f to estimate the wave speed [11, e.g.], we follow the work of Bramson [4] on the Fisher–KPP equation (see also Nolen et al. [19]), who showed

that the wave speed is approached only logarithmically as $t \to \infty$. Correspondingly, we expect that a constant wave speed is approached according to

$$x_f(t) \sim ct + k_0 \log(t) + k_1, \qquad t \to \infty, \tag{7}$$

where c is the wave speed, and k_0 and k_1 are constants; k_1 depends on the initial condition, and while $k_0 = -3/2$ for the minimum-speed Fisher–KPP solution, it likely depends on the parameters for the more complex model (5). To estimate c we thus fit the nonlinear relationship (7) for large times. We find that including this logarithmic correction improves the estimate of the long-time wave speed.

In Fig. 1 we plot typical results (profiles of u and v over time) for a combination of different cell death rates γ and initial conditions. In Fig. 1(a,b), we consider an initially compactly supported invading cell population:

$$u_0(x) = \begin{cases} 1 & x < 1 \\ 0 & x \geq 1 \end{cases}, \qquad v_0 = 0.5,$$

for the values $\gamma = 1$ and $\gamma = 10$, respectively. It is apparent from examining the behaviour of solutions that the system is tending toward a travelling wave of fixed shape and constant speed. Using the method described above, we estimate the wave speed of each of these cases to be $c = 1.00$ and $c = 1.24$, respectively. In Figs. 1(c,d) we consider initial conditions with exponential decay, and larger initial resident cell population:

$$u_0(x) = e^{-ax}, \qquad v_0 = 0.75,$$

for $a = 0.27$ and $a = 0.21$, respectively, and again for $\gamma = 1$ and $\gamma = 10$, respectively. These decay rates a have been chosen so that 1(c) has the same long-time wave speed as 1(a), and 1(d) has the same long-time wave speed as 1(b). A linear analysis near the front, as carried out in El-Hachem et al. [11], and also below in Sect. 3, predicts that for an exponentially decaying initial condition $u_0(x) = \exp(-ax)$, the wave speed is given by

$$c = \begin{cases} 2(1 - v_0) & a \geq 1 \\ \left(a + \frac{1}{a}\right)(1 - v_0) & a < 1, \end{cases} \tag{8}$$

which motivates the choice of initial conditions above (we will see, however, that (8) only holds for sufficiently small γ). What is important to note in Fig. 1 is that the wave speed is dependent on both the parameter γ and the initial conditions of u and v, and, indeed, two different sets of initial conditions for the same value of γ can result in the same wave speed c.

To further explore the possible behaviour of the system (5), we run simulations and estimate travelling wave speeds for a much wider range of parameter values and initial conditions. For compactly supported $u_0(x)$, we estimate the wave speed for values of γ ranging from 0.1 to 10^6, and for values $v_0 \in \{0.25, 0.5, 0.75\}$. These estimated wave
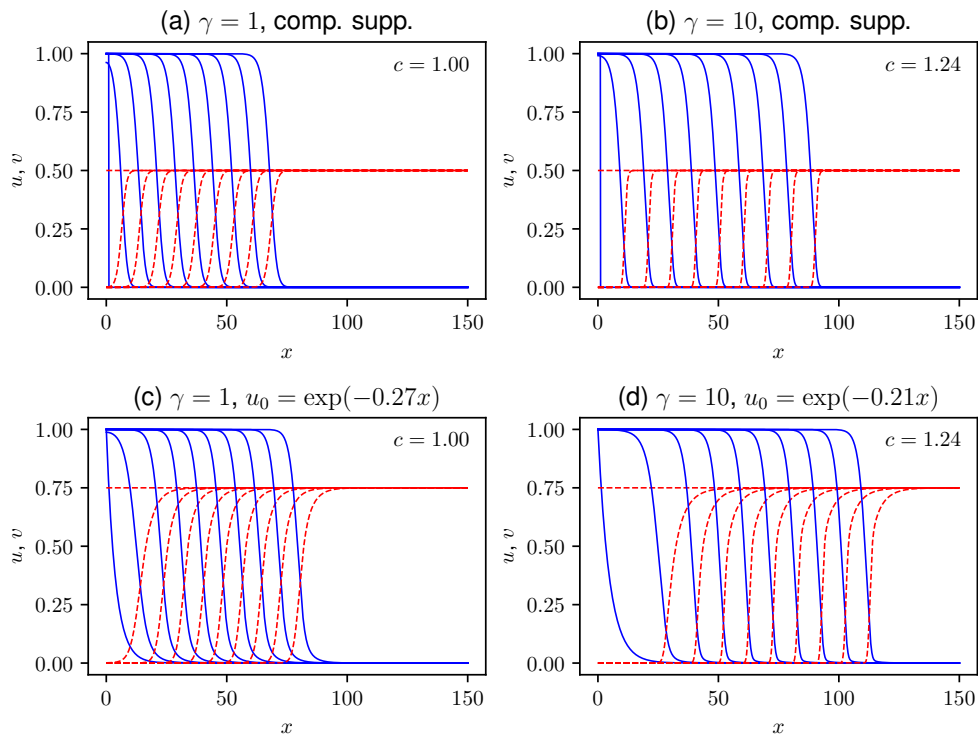
6

Figure 1: Numerical solutions of the PDE system (5), with various initial conditions and parameter values. In (a, b), $v_0 = 0.5$ and u_0 is compactly supported, while $\gamma = 1, 10$, respectively. In (c, d), $v = 0.75$ and $u_0(x) = \mathrm{e}^{-ax}$ is an exponentially decreasing initial condition, where the value of a has been chosen specifically to result in the same wave speed as for the results in (a) and (b), respectively. The estimated wave speed c (from (7)) is noted in each simulation.
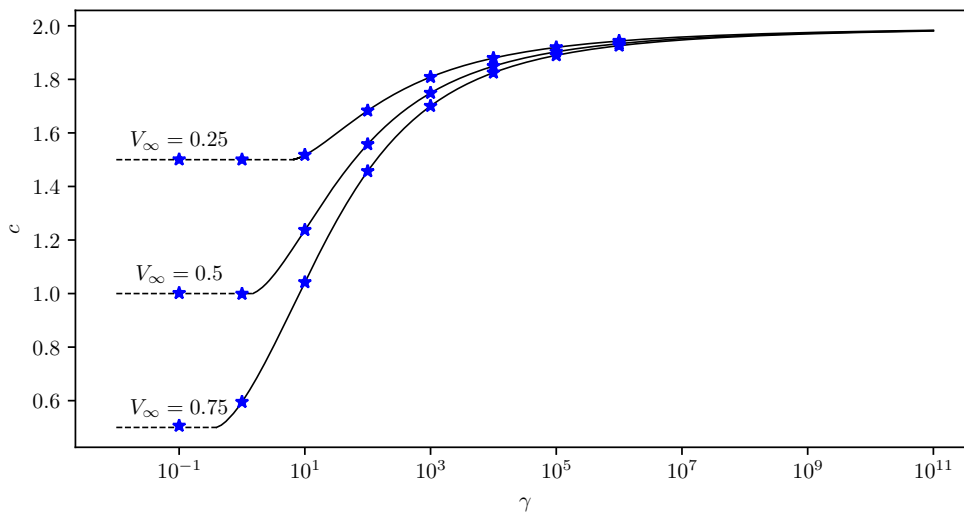
Figure 2: The dependence of wave speed c on death rate γ, for different values of initial resident cell population $v_0 = V_\infty$. Blue symbols indicate the estimation of wave speed from PDE simulations described in Sect. 2. The dashed curves represent the predicted wave speed according to the condition that $V_\infty = V_c$ (12), while the solid curves represent the predicted wave speed according to the condition $V_\infty = V_s$, where V_s must be found by numerically solving the system (9). The PDE simulations with initial condition $v_0 = V_\infty$ predict the same wave speed as the travelling wave analysis.

speeds are plotted in Fig. 2, and will be used to validate the predictions made from the direct computation of travelling wave solutions in the next section. The most notable property of these speeds is that for sufficiently small γ, the wave speed is given by $c = 2(1 - v_0)$ independent of γ, while for sufficiently large γ, the wave speed becomes dependent on γ. The point of transition between these behaviours depends on v_0, but in all cases, as $\gamma \to \infty$, the speed c approaches 2 from below.

We test the effect of initial condition of u by calculating the wave speed for $\gamma \in [0.1, 10^6]$, fixed $v_0 = 0.5$, and exponentially decaying initial conditions $u_0 = e^{-ax}$ for $a \in \{0.5, 0.325, 0.25\}$. These wave speeds are plotted in Fig. 3. These results show that for sufficiently small a and γ, the wave speed is given by the formula (8). Furthermore, for a fixed a sufficiently small such that the wave speed c is greater than 2, that is

$$a > a^* = \frac{1}{1 - v_0} - \sqrt{\frac{1}{(1 - v_0)^2} - 1},$$

the wave speed is given by (8) for any γ. The value $a = 0.25$ shown in Fig. 3 satisfies this condition. On the other hand, if $a < a^*$, for sufficiently large γ the wave speed is the same as the γ-dependent wave speed of the compactly supported initial condition. Equivalently, for a fixed γ, as a is increased, the wave speed is ultimately limited by the corresponding wave speed of the compactly supported initial condition of the same
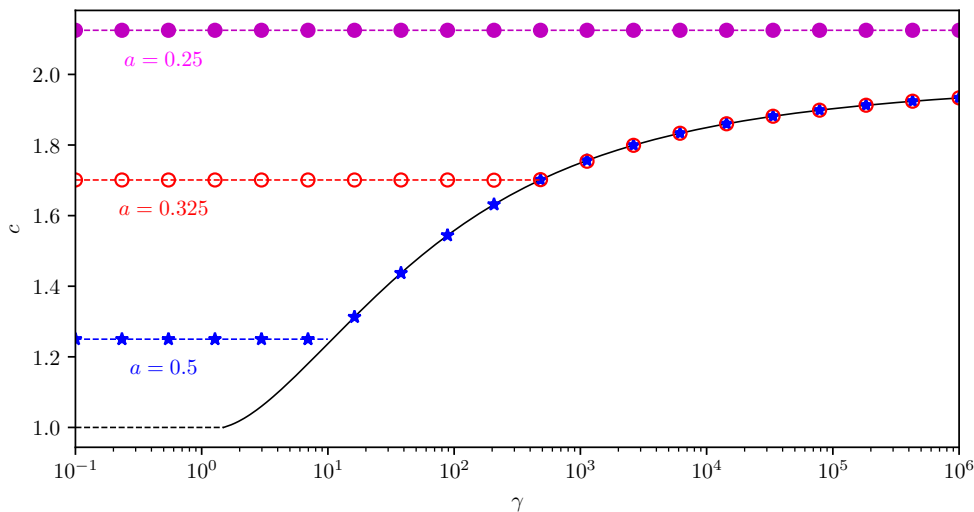
8

Figure 3: The dependence of wave speed c on death rate γ, for initial resident cell population $v_0 = 0.5$ and different invading cell initial conditions $u_0 = \exp(-ax)$, for $a \in \{0.5, 0.325, 0.25\}$. The wave speed predicted by the formula (8) is depicted by the coloured dashed lines. The wave speed of a compactly supported initial condition, corresponding to that in Fig. 2, is shown as black dashed/solid lines.

value of γ. In the next section we explain this phenomenon via the calculation of travelling wave solutions in phase space.

3   Calculation of travelling wave solutions

In this section we will compute the travelling wave solutions to (5). Let $z = x - ct$ be the travelling wave coordinate, and let $u(x,t) = U(z)$, $v(x,t) = V(z)$, and $u_x(x,t) = U'(z) = W(z)$. The system of PDEs then becomes the system of three autonomous differential equations:

$$U' = W \tag{9a}$$

$$V' = \frac{\gamma}{c}UV \tag{9b}$$

$$W' = \frac{1}{1-V}\left(\frac{\gamma}{c}UVW - cW - U(1 - U - V)\right). \tag{9c}$$

This system (9) has an isolated equilibrium at $(U, V, W) = (1, 0, 0)$. In addition, each point on the V-axis $(U, V, W) = (0, V_\infty, 0)$ is an equilbrium, each of which is therefore not isolated. Travelling wave solutions correspond to heteroclinic orbits connecting $(1, 0, 0)$ (as $z \to -\infty$) to a point on the V-axis (as $z \to \infty$). The travelling wave

9

solution relevant to an initial value problem to (5) with $v(x, 0) = v_0$ is one in which this point on the V-axis has $V_\infty = v_0$.

The eigenvalues and eigenvectors of $(1, 0, 0)$ are

$$\lambda_1 = \frac{\gamma}{c}, \quad \lambda_2 = \frac{-c + \sqrt{c^2 + 4}}{2}, \quad \lambda_3 = \frac{-c - \sqrt{c^2 + 4}}{2}. \tag{10a}$$

$$\boldsymbol{E}_1 = \begin{bmatrix} 0 \\ 1 \\ 0 \end{bmatrix}, \quad \boldsymbol{E}_{2,3} = \begin{bmatrix} 1 \\ 0 \\ \lambda_{2,3} \end{bmatrix}. \tag{10b}$$

This equilibrium thus has a two-dimensional unstable manifold. At the other end, the eigenvalues near a point $(0, V_\infty, 0)$ are

$$\lambda'_1 = 0, \quad \lambda'_2 = -\mathcal{C} + \sqrt{\mathcal{C}^2 - 1}, \quad \lambda'_3 = -\mathcal{C} - \sqrt{\mathcal{C}^2 - 1}, \quad \mathcal{C} = \frac{c}{2(1 - V_\infty)}, \tag{11}$$

with eigenvectors

$$\boldsymbol{E}'_1 = \begin{bmatrix} 0 \\ 1 \\ 0 \end{bmatrix}, \quad \boldsymbol{E}'_{2,3} = \begin{bmatrix} \lambda'_{2,3} \\ \gamma V_\infty / c \\ (\lambda'_{2,3})^2 \end{bmatrix}.$$

The zero eigenvalue λ'_1 (with eigenvector pointing along the V-axis) is due to the non-isolated nature of each fixed point. The other two eigenvalues are negative, indicating that trajectories are attracted to the V-axis in its neighbourhood. As there is one degree of freedom in trajectories leaving $(1, 0, 0)$, there is a one-parameter family of trajectories that connect $(1, 0, 0)$ to the V-axis, each ending at a different value of V_∞ between 0 and 1.

In Colson et al. [7] trajectories of their similar system were found via a shooting algorithm. Here we compute solutions of (9) numerically by solving it as a boundary value problem on a large domain $z \in (0, z_\infty)$, using the numerical continuation package AUTO-07p [9]. This will allow us to compute solutions for more extreme values of parameters (in particular γ). Appropriate boundary conditions are

$$U(0) = 1 + \varepsilon, \quad W(0) = -\epsilon \lambda_2, \quad V(z_\infty) = V_\infty$$

where ε is a small parameter, and $z_\infty \gg 1$. These boundary conditions enforce that near $(1, 0, 0)$, trajectories are on the eigenvector with the smaller positive eigenvalue. For a given γ and c we are able to construct travelling wave solutions for any value of V_∞ between 0 and 1, by starting at $V_\infty = 0$ (at which point V vanishes identically, and U, W are solutions to the Fisher–KPP system), and then increasing V_∞ by numerical continuation.

We plot examples of such trajectories, projected onto the (U, V) plane, in Fig. 4. In this figure we choose two sets of parameters $(\gamma, c) = (1, 1)$ and $(10, 1.24)$ in order to
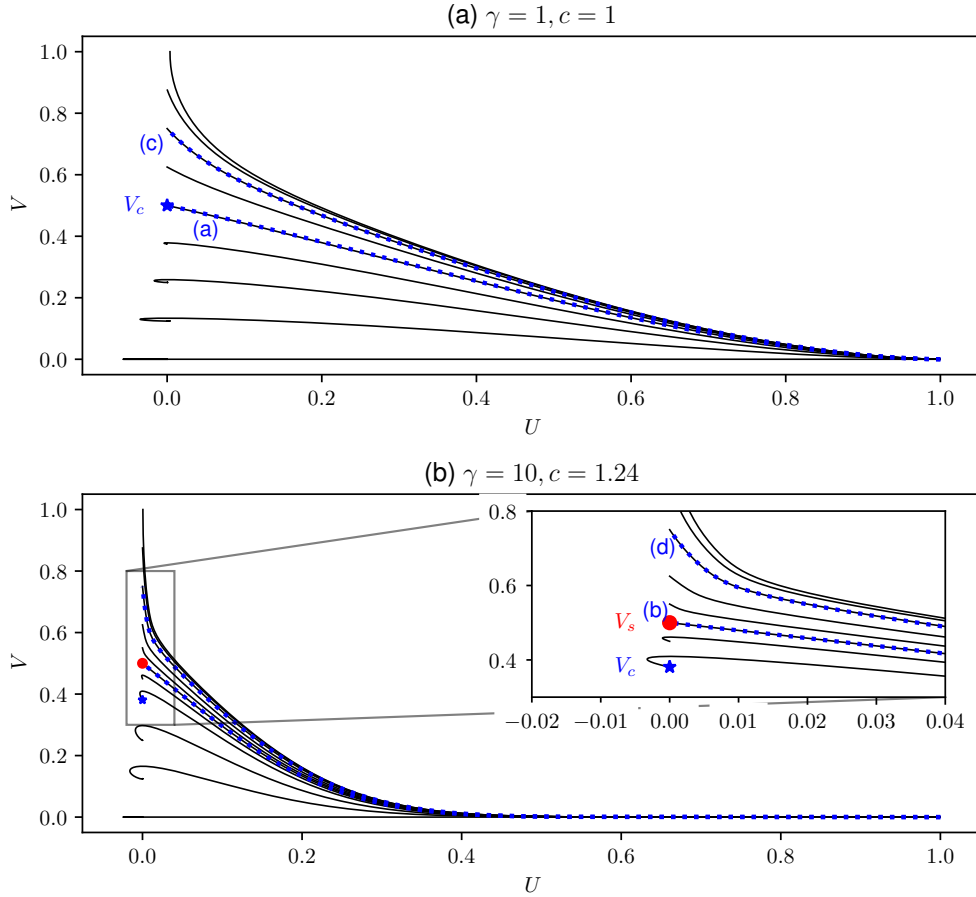
10

Figure 4: Trajectories in (U, V, W) phase space, projected onto the (U, V) plane, for (a) $(\gamma, c) = (1, 1)$ and (b) $(\gamma, c) = (10, 1.24)$. In (a), the parameters are such that trajectories spiral into the V-axis for $V < V_c$, and monotonically approach the V-axis for $V \geq V_c$. In (b), there is also a critical value V_s such that U approaches zero from below when $V < V_s$ and above when $V > V_s$. Dotted curves marked (a)–(d), corresponding to the late-time PDE simulations depicted in Figs. 1a–d, respectively, show that PDE simulations are attracted to travelling wave solutions with either the same decay rate as initial condition (if such a solution exists), or to the travelling wave with fastest decay rate, at $V_\infty = \max\{V_c, V_s\}$.

compare to the travelling wave solutions observed in the PDE simulations shown in Fig. 1.

For given values of γ and c, there is a one-parameter family of travelling wave solutions, that we may consider as characterised by the value V_∞. Since the wave speed c is a parameter of the system, we thus expect that for a given V_∞ there is a one-parameter family of travelling wave solutions, parametrised by c, and it is not yet apparent which travelling wave solution will correspond to the long-time behaviour of a solution to the PDE system (5) for a given initial condition. In order to determine this wavespeed selection, we need to consider the behaviour of trajectories near the front of the travelling wave, that is, near the V-axis. Firstly, we note that for a given wavespeed c, there is a critical value $V = V_c$, at which the eigenvalues $\lambda'_{2,3}$ switch from complex to real:

$$V_c = 1 - \frac{c}{2}. \tag{12}$$

This value is independent of the decay rate γ. Trajectories for which $V_\infty < V_c$ spiral into the relevant point on the V-axis, and since this corresponds to negative values of U, such trajectories cannot correspond to solutions to (5) that have evolved from a non-negative initial condition. This property is determined locally, and is equivalent to the condition used to determine the minimum wave speed in the Fisher–KPP equation.

However, it is not always the case that U is positive on trajectories for which $V_\infty > V_c$. This is true in particular when γ is sufficiently large. In Fig. 4(b) (in particular the inset of that figure) in which $\gamma = 10$, we observe that trajectories for which V_∞ is slightly larger than V_c still approach the V-axis from the negative ($U < 0$) side, despite the fact that eigenvalues are real at these points. In this parameter regime there is a point V_s (indicated as a red dot in Fig. 4(b)) that separates trajectories that have U become negative, from those that remain positive. The existence of such a threshold value was also noted in the similar model of Colson et al. [7]. Unlike the point V_c, the point V_s is not determined as a local property of the phase space (it is a property of the manner in which the unstable manifold of $(1, 0, 0)$ intersects the V-axis), so is unlikely to have a closed-form expression.

We may understand the existence of this critical point V_s by considering the linearisation near the V-axis. For $V_c < V_\infty < 1$, a trajectory near the V-axis will behave as

$$\begin{bmatrix} U \\ V \\ W \end{bmatrix} \sim \begin{bmatrix} 0 \\ V_\infty \\ 0 \end{bmatrix} + r_2 \boldsymbol{E}'_2 \mathrm{e}^{\lambda'_2 z} + r_3 \boldsymbol{E}'_3 \mathrm{e}^{\lambda'_3 z}, \qquad z \to \infty, \tag{13}$$

where $\lambda'_{2,3}$ and $\boldsymbol{E}'_{2,3}$ are the eigenvalues and eigenvectors (11). For $V > V_c$, $\lambda'_3 < \lambda'_2 < 0$, so that the generic case is that $U \to 0$ with decay rate given by the less negative eigenvector λ'_2. The magnitudes of one of the constants r_2 and r_3 is arbitrary due to translational invariance, but these constants are otherwise unique properties of a given trajectory. Importantly, a trajectory may have $r_2 > 0$, which means that (for the

eigenvector written as in (11)) the trajectory approaches the V-axis from the negative U direction. These are the trajectories observed in Fig. 4(b) for $V_c < V_\infty < V_s$. These trajectories also cannot correspond to a travelling wave solution of (5) reached from a non-negative initial condition. The critical point V_s represents the end point of the particular trajectory at which the coefficient r_2 in (13) goes from being positive to negative, that is, at $V_\infty = V_s$, $r_2 = 0$. What is special about this point then is that $U \to 0$ with decay rate given by the *more negative* eigenvalue λ_3'. In other words, for parameter values in which a point V_s exists, the trajectory ending at V_s (rather than V_c) is the travelling wave solution with the greatest decay as $z \to \infty$.

Trajectories that end at $V_\infty > \max\{V_c, V_s\}$ are also valid travelling wave solutions that exhibit a specific exponential decay. Indeed, when we plot the curves in the (U, V) plane that correspond to the late-time PDE simulations (see Fig. 4), we see that these exactly correspond to trajectories on the phase plane, terminating either at V_c or V_s (for the compactly supported initial conditions), or at a higher value (for the slowly exponentially decaying initial condition). Identifying the eigenvalue λ_2' from (11) with $-a$, a travelling wave solution will have decay rate a given that the wave speed (8) holds (which is how that formula is derived). However, as observed in the PDE simulations depicted in Fig. 3, for sufficiently large a, the wave speed is replaced by that corresponding to a compactly supported initial condition. This is because a trajectory may only end at a given V_∞ when $V_\infty > \max\{V_c, V_s\}$ for the given wave speed and value of γ. For sufficiently large a, the wave speed will be limited either by the existence of V_c, so that

$$c = 2(1 - V_\infty), \tag{14}$$

or by the existence of V_s, in which case c will be the value such that $v_0 = V_s$ for given (γ, c).

We calculate the location of V_s in our numerical continuation procedure by tracking the value of $U(z_\infty)$. While in the limit $z_\infty \to \infty$ this value will vanish, for a finite $z_\infty < \infty$ it is generally small but nonzero. In this case, the value of V_∞ where $U(z_\infty) = 0$ corresponds (closely enough for the computations) to the threshold value $V_\infty = V_s$. Using numerical continuation we are then able to fix $U(z_\infty) = 0$ and allow γ and c to vary, for a given V_∞. The parameter γ can then be increased to very large values, for which the wave speed slowly approaches 2. As γ is decreased, eventually V_s collides with the other critical point V_c.

Using this procedure we produce curves of wave speed c as a function of γ, for given values of the far-field resident cell population V_∞. These results are plotted in Fig. 2 along with the estimates from the PDE simulations for compactly supported initial conditions. When γ is sufficiently small such that V_s does not exist, we instead use the condition that $V_\infty = V_c$, thus $c = 2(1 - V_\infty)$. The comparison confirms that we have correctly identified the wave speed selection mechanism.

As we can explicitly calculate travelling wave solutions, we are able to continue to

much larger values of γ than would be feasible if we relied only on PDE simulations. We observe in Fig. 2 that in the limit that γ becomes large, the wave speed tends to a constant value 2, but does so very slowly. Example travelling wave profiles are shown for $V_\infty = 0.5$, and $\gamma \in \{10, 10^5, 10^{11}\}$, in Fig. 5. These profiles highlight that as γ increases, the travelling wave solutions exhibit a region in which both cell populations are very small, and this region grows, but again slowly, as $\gamma \to \infty$. This region corresponds to the hypocellular interstitial gap described in Gatenby and Gawlinski [15]. In the next section we carry out the matched asymptotic analysis in this limit, which will explain the logarithmic dependence on γ of both the wave speed and the interstitial gap width.

4   Large death rate asymptotic analysis

In this section we describe the asymptotic analysis of the relation between resident cell death rate γ and wave speed c in the limit that γ becomes large. We restrict ourselves to the travelling wave branches that correspond to compactly supported initial conditions (that is, $V_\infty = V_s$ in the preceding section).

The important observation is that for large γ, (9b) implies that V is asymptotically small except near the front (where $V \to V_\infty$ as $z \to \infty$). The effect of γ is thus to modify the leading order, Fisher–KPP solution, a property that was observed in PDE simulations in El-Hachem et al. [11]. In addition, this phenomenon is very similar to that which occurs when the Fisher–KPP system is modified by a small cut-off factor in the reaction term (3), as considered in Brunet and Derrida [6] and Dumortier et al. [10]. Our asymptotic analysis will follow along similar lines to Brunet and Derrida [6]. We will also numerically determine the prefactors in the leading order asymptotic approximations, which are required to observe the effect of V_∞ on the asymptotic wave speed.

4.1   Outer and intermediate regions

Let $\gamma \gg 1$ and let the wave speed $c = 2 - \delta$, where $\delta \to 0$ as $\gamma \to \infty$ is the correction to the wave speed. In the limit $\gamma \gg 1$, (9b) implies that $V = 0$ to leading order, so that to leading order, U and W are given by travelling wave solutions to the Fisher–KPP system (1) with wavespeed $c = 2$:

$$U \sim U_0(z), \qquad W \sim W_0(z), \qquad \delta \to 0, \qquad z - z_0 = O(1) \qquad (15)$$

where

$$U_0' = W_0, \qquad W_0' = -2W_0 - U_0(1 - U_0), \qquad \lim_{z \to -\infty}(U_0, W_0) = (1, 0). \qquad (16)$$
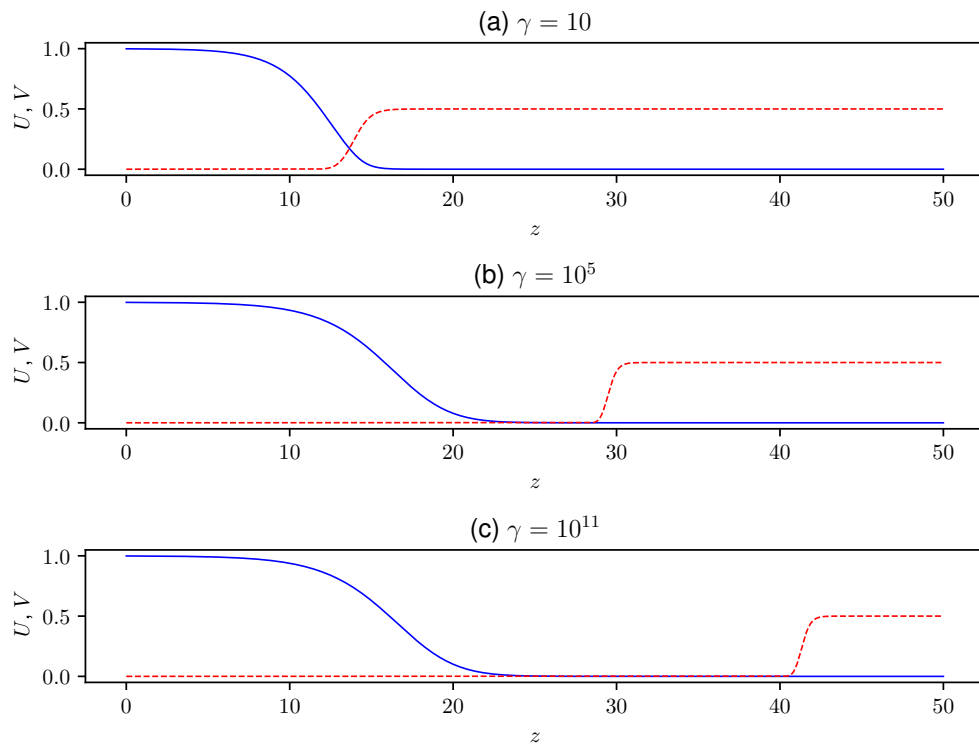
14

Figure 5: Travelling wave solutions for U (blue solid curves) and V (red dashed curves), for $V_\infty = 0.5$ and (a) $\gamma = 10$, (b) $\gamma = 10^5$, and (c) $\gamma = 10^{11}$. The interstitial gap (the region in which both cell populations are small) is seen to grow slowly; the asymptotic analysis of Section 4 predicts this region is of order $\log \gamma$ as $\gamma \to \infty$.

As $z \to \infty$, the behaviour of this leading order solution is determined by the repeated eigenvalue of the Fisher–KPP system near the origin:

$$U_0 \sim A_0(z - z_0)e^{-(z-z_0)}, \qquad z \to \infty. \tag{17}$$

In (17) we have explicitly written the arbitrary constant of translation z_0. In this form the prefactor A_0 is not arbitrary, but is a constant that is a property of the unique solution to (16). The numerical value of A_0 may be found by computing the value of

$$\log(A_0) = \lim_{z \to \infty} \ell(z), \qquad \ell(z) = \frac{U_0}{U_0 + W_0} + \log |U_0 + W_0|. \tag{18}$$

By solving (16) numerically and using the formula (18), we determine that

$$A_0 \approx 0.1419. \tag{19}$$

As z increases, the system (9) reaches an intermediate region in which the effect of subcritical wave speed ($\delta > 0$) becomes important. Since this effect is to reduce the wave speed below the critical value 2, the leading order Fisher–KPP approximation is pushed into the regime in which the origin is a stable spiral. That is,

$$U \sim U_M, \qquad (2 - \delta)U_M' + 2U_M'' + U_M, \tag{20}$$

with solution (matching to the outer solution (17))

$$U_M = A_0\delta^{-1/2}e^{-(z-z_0)} \sin\left(\delta^{1/2}(z - z_0)\right). \tag{21}$$

This asymptotic behaviour holds when $\delta \to 0$ with $z - z_0 = O(\delta^{-1/2})$. It is this intermediate behaviour that must be matched to the inner region in which V is no longer small.

4.2   Inner problem and matching

In the inner region, U and W are small, and $V = O(1)$. Let $U = \gamma^{-1}\hat{U}$, $W = \gamma^{-1}\hat{W}$. To leading order in this inner region, the system (9) is

$$\hat{U}' = \hat{W}, \quad V' = \frac{1}{2}\hat{U}V, \quad \hat{W}' = \frac{1}{1 - V}\left(\frac{1}{2}\hat{U}V\hat{W} - 2\hat{W} - \hat{U}(1 - V)\right). \tag{22}$$

Considering solutions for which $V_\infty = V_s$, the relevant inner boundary condition is that the trajectory approaches the given $V = V_\infty$ along the more negative eigenvector, that is,

$$\begin{bmatrix} \hat{U} \\ V \\ \hat{W} \end{bmatrix} \sim \begin{bmatrix} 0 \\ V_\infty \\ 0 \end{bmatrix} + \begin{bmatrix} \Lambda \\ V_\infty/2 \\ \Lambda^2 \end{bmatrix} e^{\Lambda z}, \quad z \to \infty, \tag{23}$$

16

where
$$\Lambda = -\frac{1}{1 - V_\infty}\left(1 + \sqrt{1 - (1 - V_\infty)^2}\right) \tag{24}$$

is the leading order $(c \to 2)$ eigenvalue corresponding to λ_3' in (11).

This inner problem is too intractable to solve in closed form. However, we only require the far field $(z \to -\infty)$ behaviour of these solutions to match to the intermediate region (21). As $z \to -\infty$, $V \to 0$ and the leading order inner problem (22) approaches the linearised version of the critical-speed Fisher–KPP equation near the origin, that is

$$\hat{W}' \sim -2\hat{W} - \hat{U}, \qquad \hat{U}' = \hat{W}, \qquad z \to -\infty.$$

Thus, similar to the outer problem,

$$\hat{U} \sim -A_I(z - z_I)\mathrm{e}^{-(z - z_I)}, \qquad z \to -\infty. \tag{25}$$

Again z_I is arbitrary due to the translational invariance of (22), but the constant A_I depends in a nontrivial way on the entire solution to (22), and thus on V_∞. With the sign convention in (25), A_I will be positive. By integrating (22) numerically in the negative z direction, from an initial condition (23), we may numerically compute A_I independently of z_0 in a similar way as to the Fisher–KPP system, by computing

$$\log(A_I) = \lim_{z \to -\infty} \frac{\hat{U}}{\hat{U} + \hat{W}} + \log|\hat{U} + \hat{W}|.$$

For the typical values of $V_\infty \in \{0.25, 0.5, 0.75\}$ we have considered thus far, we use this expression to estimate

$$A_I|_{V_\infty = 0.25} \approx 0.515, \qquad A_I|_{V_\infty = 0.5} \approx 1.485, \qquad A_I|_{V_\infty = 0.75} \approx 2.943. \tag{26}$$

In order for the inner solution (25) to match to the intermediate region (21), the sinusoidal term in the intermediate solution must approach zero, which happens when its argument is in the neighbourhood of π. We define a new spatial variable ξ by $z - z_0 = \delta^{-1/2}\pi + \xi$. In matching we then require $z_I = z_0 + \delta^{-1/2}\pi$, and

$$-A_0 \mathrm{e}^{-\pi\delta^{-1/2}}\xi\mathrm{e}^{-\xi} \sim -A_I \gamma^{-1}\xi\mathrm{e}^{-\xi},$$

from which we obtain the relationship between the wave speed correction δ and γ:

$$\delta \sim \pi^2\left[\log\left(\frac{A_0}{A_I}\gamma\right)\right]^{-2} \sim \frac{\pi^2}{[\log\gamma]^2} + \frac{2\pi^2\log(A_I/A_0)}{[\log\gamma]^3}. \tag{27}$$

The first term on the right hand side of (27) is equivalent to the universal correction that arises in the Fisher–KPP equation with cut-off [6, 10]. It does not depend on the specific value of V_∞, and indeed we expect it would not depend on the specifics of the

17

diffusion or reaction terms being considered, as it is purely a consequence of the fact that the intermediate problem has to match to an inner problem where U is of order γ^{-1}. In Fig. 6a we present numerical evidence that this leading order term is correct, by plotting $(\log \gamma)^{-2}$ against the correction to the velocity $\delta = 2 - c$, for the travelling wave branches we have computed for each of $V_\infty \in \{0.25, 0.5, 0.75\}$. Each of these curves is seen to approach the line with slope π^2, as predicted by the leading order term in (27). The convergence to this limit is very slow, which is unsurprising given that the asymptotic series is logarithmic in γ.

To test the correction term (the second term on the right hand side of (27)) we compute the difference between the velocity correction and the leading order term, that is

$$\delta_1 = 2 - c - \frac{\pi^2}{[\log \gamma]^2},$$

and, in Fig. 6b, plot this quantity as a function of $(\log \gamma)^{-2}$, along with the asymptotic prediction. The asymptotic prediction depends on V_∞ through A_I, so is different for each branch. This comparison confirms that the correction term improves the estimate in the limit $\gamma \to \infty$, but again highlights the very slow convergence of the asymptotic approximation in this limit.

Finally, we note that in the intermediate region in which U behaves as (21), both U and V are small. This region therefore corresponds to the interstitial region that can be observed in Fig. 5. The asymptotic analysis predicts that the width of this region is $O(\delta^{-1/2}) = O(\log \gamma)$, hence the slow growth of this region in the large γ limit.

5 Discussion

In this article we have determined the properties of the three dimensional phase space that select the wave speed of the system (5) for compactly supported or exponentially decaying initial conditions. Although the phase-space properties of the three-dimensional system in travelling wave coordinates (9) are more complicated than the two-dimensional Fisher–KPP system, the general principle of wave speed selection is the same. For an initial condition of given far field exponential decay, a PDE solution will evolve toward the travelling wave solution which has the same decay rate, if such a nonnegative solution exists. Otherwise, the solution will tend to the travelling wave solution which has the largest decay rate. Depending on the value of γ and v_0, the solution with fastest decay rate will either correspond to the wave speed c such that $v_0 = V_c$, or such that $v_0 = V_s$, if that point exists. An important point regarding the determination of V_s is, although it is a property of the phase space, it is not a local property in the neighbourhood of the V-axis; rather, it is related to the manner in which the two-dimensional unstable manifold of $(U, V, W) = (1, 0, 0)$ intersects the
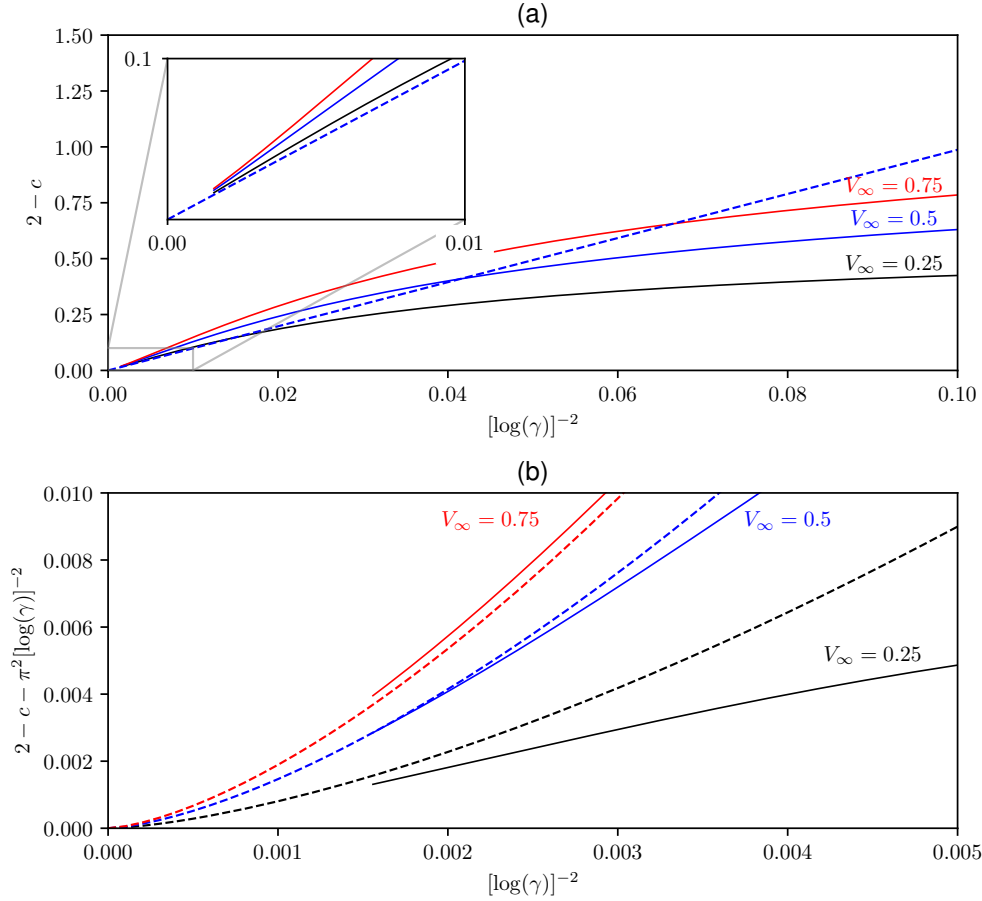
Figure 6: Comparison between the numerically determined travelling wave speeds and the asymptotic approximation for large γ. (a) Comparison between the wavespeed correction $\delta = 2 - c$ and numerically determined values and the leading order term in (27) show convergence to the leading order universal logarithmic behaviour that is independent of V_∞. (b) Comparison between the next term in the asymptotic approximation (27), in which the effect of V_∞ plays a role.

V-axis. For this reason, the existence or location of V_s cannot be determined by a local expansion, so there is unlikely to be a general closed-form expression for the selected wave speed.

We have also performed the asymptotic analysis of travelling waves in the large γ limit. In carrying out this limit it is useful to think of the system as a generalisation of the Fisher–KPP system in which the reaction term is perturbed, leading to a logarithmically small correction to the wave speed from the critical Fisher–KPP wave speed of 2. The leading order correction in this case is universal, so is likely to be the correction observed for a large class of systems that look like (5) with variations in diffusivity and reaction terms; for example, the system considered by Colson et al. [7], in which the resident cell population effects the diffusivity but not the reaction, is likely to have the same leading order asymptotic behaviour.

In this work we have not considered the degenerate-diffusion case where $v_0 = 1$ (or $V_\infty = 1$ in calculating travelling wave solutions). In this case, as discussed in El-Hachem et al. [11] and in the closely related problem in Colson et al. [7], the appropriate trajectories end at the point $(U, V, W) = (0, 1, 0)$, which is a removable singularity in the phase space (as it is the intersection of the V-axis and the plane $V = 1$), rather than a fixed point. Travelling waves therefore do not behave exponentially near this point. A local expansion will give the permitted behaviour near this point; one method of recovering this is to desingularise the system (9) and perform a centre manifold analysis, similar to that considered in Gallay and Mascia [14], for example. It is unclear if, in this case, the selected wave speed c (corresponding to a compactly supported initial condition) will be selected by a mechanism similar to that which determines the point V_s: that is, out of all trajectories over c that end at $(0, 1, 0)$, there will be a unique trajectory such that the decay is maximum. We note that the PDE simulations in El-Hachem et al. [11] suggest that the wavespeed at $v_0 = 1$ is also the one approached if one takes the limit as $v_0 \to 1$ from below, which indicates that the wave speed selection mechanism should be related.

References

[1] D.G. Aronson and H.F. Weinberger. Nonlinear diffusion in population genetics, combustion, and nerve pulse propagation. In J. A. Goldstein, editor, *Partial Differential Equations and Related Topics: Ford Foundation Sponsored Program at Tulane University, January to May, 1974*, volume 446, pages 5–49. Springer, 1975.

[2] D.G. Aronson and H.F. Weinberger. Multidimensional nonlinear diffusion arising in population genetics. *Adv. Math.*, 30:33–76, 1978. doi:10.1016/0001-8708(78)90130-5.

[3] E. Boedtkjer and S.F. Pedersen. The acidic tumor microenvironment as a driver

of cancer. *Ann. Rev. Phys.*, 82(1):103–126, 2020. doi:10.1146/annurev-physiol-021119-034627.

[4] M. Bramson. *Convergence of solutions of the Kolmogorov equation to travelling waves*, volume 44. American Mathematical Soc., Providence, RI., 1983.

[5] A.P. Browning, P. Haridas, and M.J. Simpson. A Bayesian sequential learning framework to parameterise continuum models of melanoma invasion into human skin. *Bull. Math. Bio.*, 81:676–698, 2019. doi:10.1007/s11538-018-0532-1.

[6] E. Brunet and B. Derrida. Shift in the velocity of a front due to a cutoff. *Phys. Rev. E*, 56:2597, 1997. doi:10.1103/PhysRevE.56.2597.

[7] C. Colson, F. Sánchez-Garduño, H.M. Byrne, P.K. Maini, and T. Lorenzi. Travelling-wave analysis of a model of tumour invasion with degenerate, cross-dependent diffusion. *P. R. Soc. A.*, 477:20210593, 2021. doi:10.1098/rspa.2021.0593.

[8] P.N. Davis, P. van Heijster, R. Marangell, and M.R. Rodrigo. Traveling wave solutions in a model for tumor invasion with the acid-mediation hypothesis. *J. Dyn. Differ. Equ.*, 34:1325–1347, 2022. doi:10.1007/s10884-021-10003-7.

[9] E.J. Doedel, A.R. Champneys, F. Dercole, T.F. Fairgrieve, Yu.A. Kuznetsov, B. Oldeman, R.C. Paffenroth, B Sandstede, XJ Wang, and CH Zhang. Auto-07p. *Montreal Concordia University*, 2007. URL `http://indy.cs.concordia.ca/auto/`. http://indy.cs.concordia.ca/auto/.

[10] F. Dumortier, N. Popović, and T.J. Kaper. The critical wave speed for the Fisher–Kolmogorov–Petrowskii–Piscounov equation with cut-off. *Nonlinearity*, 20:855, 2007. doi:10.1088/0951-7715/20/4/004.

[11] M. El-Hachem, S.W. McCue, and M.J. Simpson. Travelling wave analysis of cellular invasion into surrounding tissues. *Physica D*, 428:133026, 2021. doi:10.1016/j.physd.2021.133026.

[12] A. Fasano, M.A. Herrero, and M.R. Rodrigo. Slow and fast invasion waves in a model of acid-mediated tumour growth. *Math. Biosci.*, 220:45–56, 2009. doi:10.1016/j.mbs.2009.04.001.

[13] R.A. Fisher. The wave of advance of advantageous genes. *Ann Eugenic.*, 7:355–369, 1937. doi:10.1111/j.1469-1809.1937.tb02153.x.

[14] T. Gallay and C. Mascia. Propagation fronts in a simplified model of tumor growth with degenerate cross-dependent self-diffusivity. *Nonlinear Anal. Real World Appl.*, 63:103387, 2022. doi:10.1016/j.nonrwa.2021.103387.

[15] R.A. Gatenby and E.T. Gawlinski. A reaction-diffusion model of cancer invasion. *Cancer Res.*, 56:5745–5753, 1996.

[16] F. Hamel, J. Nolen, J-M. Roquejoffre, and L. Ryzhik. A short proof of the logarithmic Bramson correction in Fisher–KPP equations. *Netw. Heterog. Media*, 8: 275–279, 2013. doi:10.3934/nhm.2013.8.275.

[17] A. Kolmogorov, I. Petrovsky, and N. Piscounov. Étude de l'équation de la diffusion avec croissance de la quantité de matière et son application à un problème biologigue. *Moscow Univ. Bull.*, 1:1–25, 1937.

[18] C. Mascia, P. Moschetta, and C. Simeoni. Numerical investigation of some reductions for the Gatenby–Gawlinski model. *Axioms*, 13:281, 2024. doi:10.3390/axioms13050281.

[19] J. Nolen, J-M. Roquejoffre, and L. Ryzhik. Convergence to a single wave in the Fisher–KPP equation. *Chinese Ann. Math. B*, 38(2):629–646, 2017. doi:10.1007/s11401-017-1087-4.

[20] S.V. Patankar. *Numerical heat transfer and fluid flow*. Taylor & Francis, 1980. ISBN 0891165223.

[21] K. Smallbone, D.J. Gavaghan, R.A. Gatenby, and P.K. Maini. The role of acidity in solid tumour growth and invasion. *J. Theor. Biol.*, 235:476–484, 2005. doi:10.1016/j.jtbi.2005.02.001.

[22] B. Swartwood. Stability analysis of traveling wave fronts in a model for tumor growth. *Nonlinear Anal—Real*, 81:104176, 2025. doi:10.1016/j.nonrwa.2024.104176.

[23] W. Van Saarloos. Front propagation into unstable states: marginal stability as a dynamical mechanism for velocity selection. *Phys. Rev. A*, 37:211, 1988. doi:10.1103/PhysRevA.37.211.

[24] W. Van Saarloos. Front propagation into unstable states. *Phys. Rep.*, 386:29–222, 2003. doi:10.1016/j.physrep.2003.08.001.